Unravelling the Superiority of Nonbenzenoid Acepleiadylene as a Building Block for Organic Semiconducting Materials

Lin Fu,[†,a] Pengcai Liu,[†,a] Rui Xue,[a] Xiao-Yu Tang,[a] Jiawen Cao,[a] Ze-Fan Yao,[b] Yuchao Liu,[c] Shouke Yan,[c] and Xiao-Ye Wang*[,a]

[a] L. Fu, Dr. P. Liu, R. Xue, X.-Y. Tang, J. Cao, Prof. Dr. X.-Y. Wang
State Key Laboratory of Elemento-Organic Chemistry, Frontiers Science Center for New Organic Matter
College of Chemistry, Nankai University, Weijin Road 94, Tianjin 300071 (China)
E-mail: xiaoye.wang@nankai.edu.cn
[b] Dr. Z.-F. Yao
Department of Chemical and Biomolecular Engineering, Samueli School of Engineering, University of California, Irvine, CA, 92697 (USA)
[c] Dr. Y. Liu, Prof. Dr. S. Yan
Key Laboratory of Rubber-Plastics (Ministry of Education), Qingdao University of Science and Technology, Qingdao 266042 (China)
[†] These authors contributed equally to this work.

Abstract: Acepleiadylene (APD), a nonbenzenoid isomer of pyrene, exhibits a unique charge-separated character with a large molecular dipole and a small optical gap. However, APD has never been explored in optoelectronic materials to take advantage of these unique properties. Here, we employ APD as a building block in organic semiconducting materials for the first time, and unravel the superiority of nonbenzenoid APD in electronic applications. We have synthesized an APD derivative (APD-IID) with APD as the terminal donor moieties and isoindigo (IID) as the acceptor core. Theoretical and experimental investigations reveal that APD-IID has an obvious charge-separated structure and enhanced intermolecular interactions as compared with its pyrene-based isomers. As a result, APD-IID displays significantly higher hole mobilities than that of the pyrene-based counterparts. These results imply the advantages of employing APD in semiconducting materials and great potential of nonbenzenoid polycyclic arenes for optoelectronic applications.

Nonbenzenoid polycyclic aromatic hydrocarbons (PAHs), which contain nonhexagonal rings, have attracted broad interest owing to their appealing topological structures, unique properties, and applications in electronic devices.[1] In recent years, a number of novel nonbenzenoid PAHs have been synthesized either in solution[2] or on metal surfaces.[3] The remarkable synthetic achievements have enabled extensive investigations of the properties of these novel compounds, such as (anti)aromaticity,[4] open-shell characters,[2g,5] and chiroptical responses.[2b,2u,6] Furthermore, as exemplified by azulene derivatives,[7] the optoelectronic applications of nonbenzenoid PAHs have also been demonstrated, e.g. in organic field-effect transistors (OFETs),[8] organic photovoltaics,[8d,9] and organic thermoelectrics.[10] However, the semiconducting properties of other nonbenzenoid PAHs beyond azulene have been rarely exploited. Besides, the advantages of nonbenzenoid PAHs over their benzenoid counterparts in optoelectronic materials have not been clearly revealed.

Acepleiadylene (APD), which is a classical nonbenzenoid PAH, features a larger molecular dipole, a smaller optical gap, and a charge-separated structure as compared with its benzenoid isomer pyrene.[11] These characters can introduce novel properties to APD-based materials. For example, the large molecular dipoles and the charge-separated structure would be conducive to strong intermolecular interactions and electronic coupling, which can lead to efficient charge transport.[8c,12] As the benzenoid isomer of APD, pyrene has been widely applied as a building block in optoelectronic materials,[13] whereas APD has never been exploited in this regard. Therefore, it is still unclear yet whether APD exhibits any superiority over pyrene in optoelectronic materials.

Herein, we employ APD as a building block in semiconducting materials for the first time. A donor-acceptor-donor (D-A-D) type molecule (APD-IID) is designed and synthesized, in which APD serves as the terminal donor moieties and isoindigo (IID) as the acceptor core (Figure 1a). Two pyrene-based isomers 1Py-IID and 2Py-IID, in which pyrenes are connected with IID at the 1- and 2-positions respectively, are synthesized for comparison. Owing to the separated charge distribution and the larger molecular dipole of APD, APD-IID exhibits more obvious charge-separated structure and stronger intermolecular interactions.[14] As a result, APD-IID shows one to two orders of magnitude higher hole mobility than that of 1Py-IID and 2Py-IID, opening up a new avenue to the future development of semiconducting materials based on nonbenzenoid PAHs.

The synthesis of APD-IID is illustrated in Figure 1b. In the presence of *N*-bromosuccinimide at room temperature, mono-brominated APD **1** was obtained in 84% yield, and was subsequently transformed to boronic ester **2** in 74% yield. A Suzuki coupling of **2** with brominated IID (**3**) afforded APD-IID in 60% yield. Thus, APD-IID was facilely synthesized in three steps with an overall yield of 37%. Meanwhile, its pyrene-based isomers, 1Py-IID and 2Py-IID, were also synthesized according to the literature[15] (see the Supporting Information). All these compounds were characterized by ^{1}H and ^{13}C NMR spectroscopies and high-resolution mass spectrometry (HRMS).

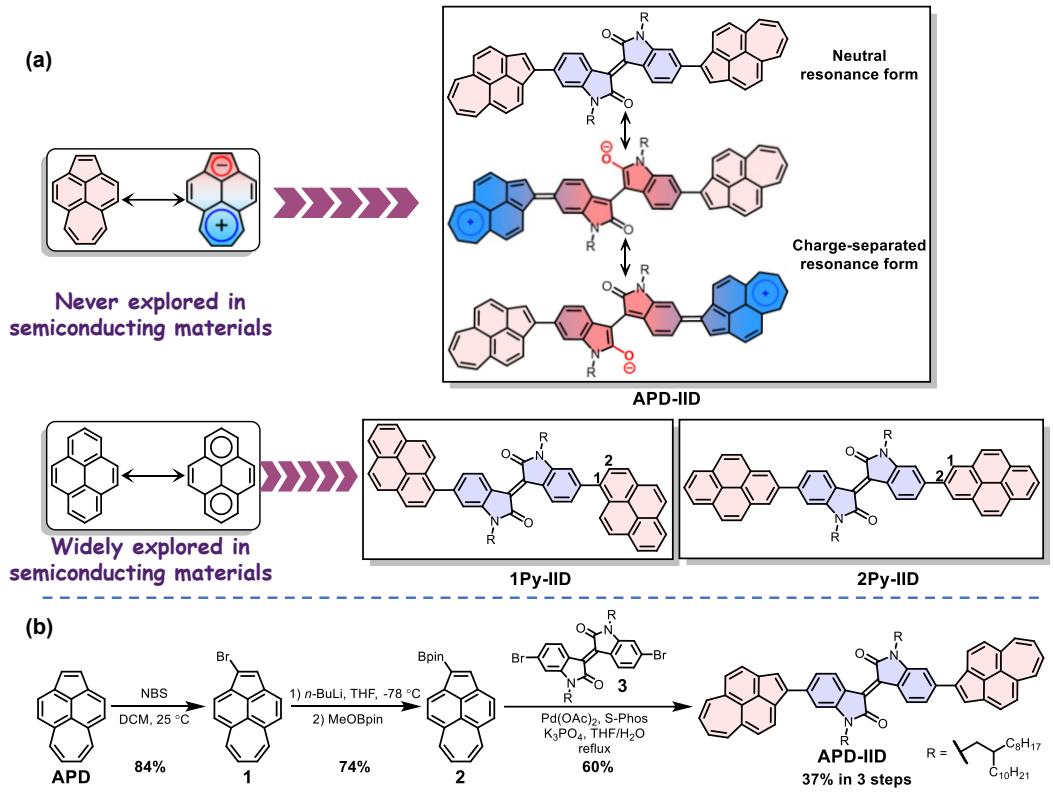

Figure 1. (a) The resonance structures of APD, pyrene and APD-IID as well as the structures of 1Py-IID and 2Py-IID. (b) Synthetic route to APD-IID.

To evaluate the molecular configurations and electronic structures of APD-IID, 1Py-IID, and 2Py-IID, density functional theory (DFT) calculations were carried out at the B3LYP/6-311G(d,p) level. As illustrated in Figure 2, the optimized geometries show that the torsion angle between the donor and acceptor moieties in APD-IID (34.9°) is smaller than that in 1Py-IID (56.7°) and 2Py-IID (38.3°), which indicates a more planar conformation of APD-IID. Meanwhile, the length of the bond that connects the donor moiety and the acceptor core in APD-IID (1.465 Å) is much shorter than that in its isomers (1.487 Å in 1Py-IID; 1.483 Å in 2Py-IID), implying that the charge-separated resonance form (Figure 1a) has a significant contribution to the electronic structure of APD-IID. As shown in the electrostatic potential (ESP) diagram (Figure 2), there is more obvious charge separation in APD-IID as compared with its pyrene-based isomers. The positive charge is mainly distributed on the seven-membered ring of APD, and the negative charge on the five-membered ring and the IID core. The charge-separated character is conducive to intermolecular electrostatic attraction in the solid state, which can provide tight molecular packing.[14] Furthermore, the highest occupied molecular orbital (HOMO) and lowest unoccupied molecular orbital (LUMO) levels of APD-IID, 1Py-IID and 2Py-IID were determined through cyclic voltammetry measurements (Figure S3 and Table S1). APD-IID exhibits a higher HOMO energy level (−5.27 eV) compared with its benzenoid isomers (−5.66 eV for 1Py-IID; −5.64 eV for 2Py-IID), indicating that APD-IID is more suitable as a *p*-type organic semiconductor.[16] In addition, these three molecules have similar LUMO energy levels (−3.67 eV for APD-IID; −3.68 eV for 1Py-IID; −3.64 eV for 2Py-IID), since their LUMO distributions are mainly localized on the IID core (Figure S11).

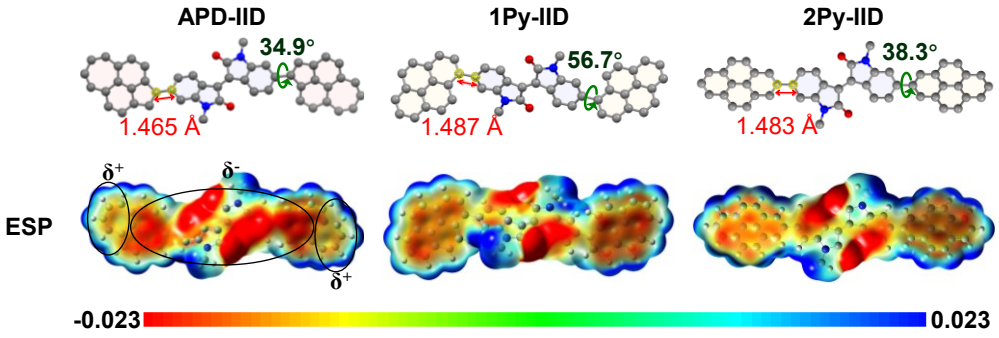

Figure 2. The optimized geometries and ESP maps for APD-IID, 1Py-IID, and 2Py-IID obtained by DFT calculations.

The UV-Vis absorption spectra of APD-IID, 1Py-IID, and 2Py-IID are shown in Figure 3. The peaks can be assigned by comparing the absorption spectra of these three molecules and their building blocks (Figure S2 and Table S1). In particular, the absorption bands at the long-wavelength region are attributed to the intramolecular charge transfer (ICT) absorption, as observed in typical donor-acceptor structures. Furthermore, the ICT band of APD-IID is much stronger than that of 1Py-IID and 2Py-IID, which illustrates the stronger ICT effect in APD-IID. Based on the lowest-energy absorption onset of the absorption spectrum, the optical gap (E_g^{opt}) of APD-IID is calculated as 1.79 eV, which is narrower than that of 1Py-IID (1.94 eV) and 2Py-IID (1.93 eV).

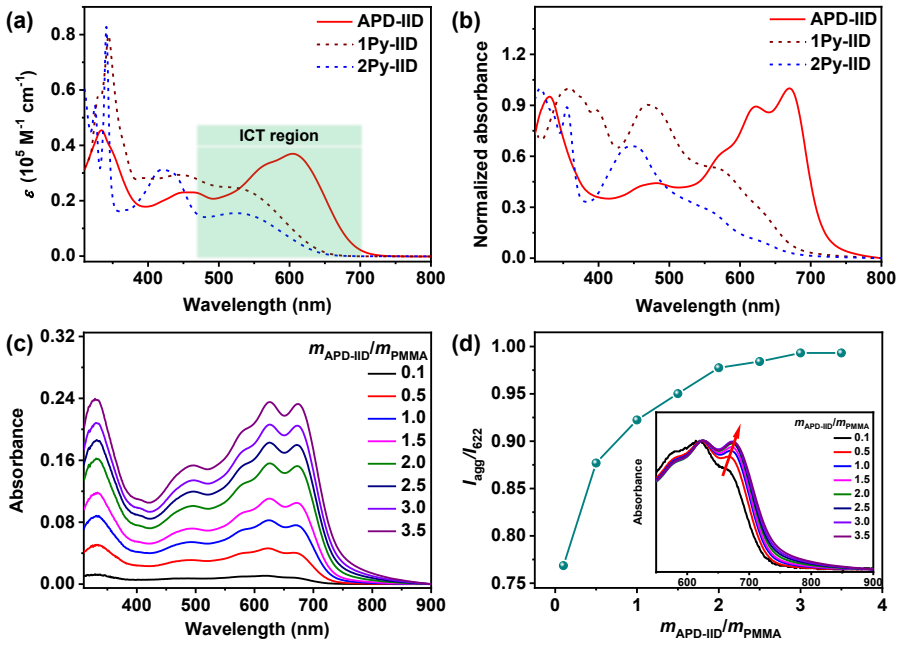

Figure 3. The UV-Vis absorption spectra of APD-IID, 1Py-IID, and 2Py-IID: (a) in toluene solutions (1×10^{-5} M) and (b) in thin films. (c) The UV-Vis absorption spectra of APD-IID in the PMMA matrix with different weight ratios ($m_{APD\text{-}IID}/m_{PMMA}$). (d) The ratios of I_{agg} and I_{622} for different $m_{APD\text{-}IID}/m_{PMMA}$ obtained from (c). Inset: the UV-Vis absorption spectra (normalized at 622 nm) of APD-IID in the PMMA matrix with different $m_{APD\text{-}IID}/m_{PMMA}$ from 550 nm to 800 nm.

The absorption spectra of APD-IID, 1Py-IID, and 2Py-IID in thin films were further characterized (Figure 3b). An apparent new shoulder peak at 670 nm was observed for APD-IID, which can be attributed to the flattening of molecular configuration caused by intermolecular aggregations (Figure S12).[17] To further study the aggregation behavior of APD-IID, 1Py-IID, and 2Py-IID in the solid state, the absorption spectra of the three molecules in the polymethyl methacrylate (PMMA) matrix with different weight ratios were recorded. As shown in Figure 3c and 3d, the aggregation peak (at around 670 nm) of APD-IID is gradually enhanced and red-shifted with increasing the $m_{APD\text{-}IID}/m_{PMMA}$ ratio, indicating a strong aggregation tendency of APD-IID in the solid state. By contrast, the absorption spectra of 1Py-IID and 2Py-IID in the thin films barely change with the increment of $m_{1Py\text{-}IID}/m_{PMMA}$ and $m_{2Py\text{-}IID}/m_{PMMA}$ (Figure S4). These results demonstrate that APD-IID has stronger intermolecular interactions in the solid state as compared with 1Py-IID and 2Py-IID.

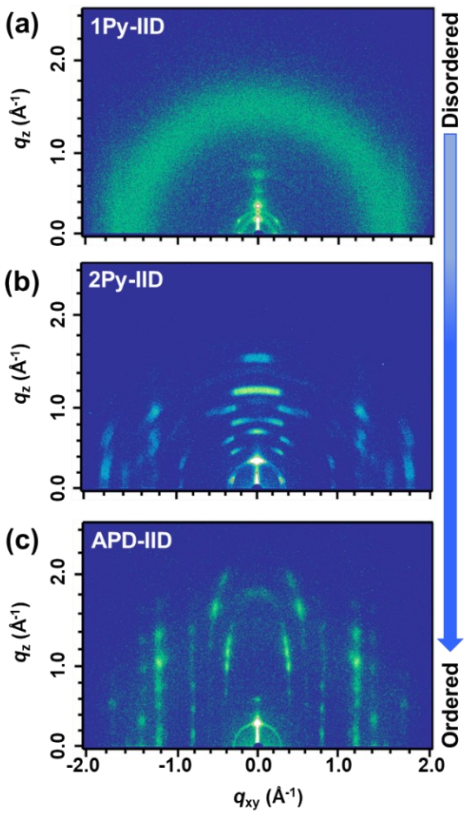

Figure 4. 2D GIWAXS images of (a) 1Py-IID; (b) 2Py-IID; (c) APD-IID thin films annealed at 90 °C.

To investigate the microstructures and morphologies of APD-IID, 1Py-IID, and 2Py-IID films, two-dimensional grazing incidence wide-angle X-ray scattering (2D GIWAXS) and atomic force microscopy (AFM) characterizations were carried out. The 2D GIWAXS images of the three molecules are qualitatively distinct. As shown in Figure 4a, 1Py-IID exhibits weak and diffused diffractions, implying its disordered packing structure. This phenomenon is consistent with the large torsion angle between the pyrene and IID moieties, as revealed by the DFT-optimized structure of 1Py-IID (Figure 2). For 2Py-IID, the 2D GIWAXS pattern shows obviously sharper diffraction arcs (Figure 4b), indicating improved packing order. By contrast, the 2D GIWAXS pattern of APD-IID displays sharp diffraction spots (Figure 4c), indicating a higher crystallinity of the thin film. Moreover, the diffraction signal along the q_z axis corresponds to the lamellar structure with a *d*-spacing of 2.1 nm, which implies that the molecules stand nearly perpendicular to the substrate with an edge-on orientation in the thin films.[18] On the other hand, AFM images of APD-IID, 1Py-IID, and 2Py-IID films exhibit smooth and continuous morphologies (Figure S10), with a root-mean-square roughness of 0.81, 0.96, and 0.93 nm, respectively.

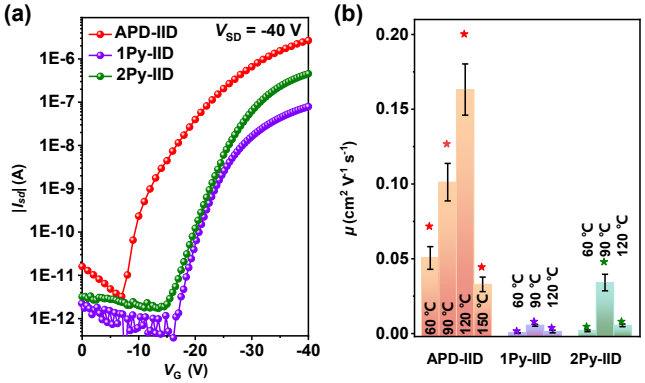

Figure 5. (a) Transfer characteristics of OFET devices based on APD-IID, 1Py-IID, and 2Py-IID. (b) Histograms of the hole mobilities extracted from the OFET devices of APD-IID, 1Py-IID, and 2Py-IID annealed at different temperatures. 30 devices are measured for each annealing temperature. The bars on the columns indicate the mean and standard deviation of the mobilities and the stars above the columns indicate the maximum values of the mobilities.

The charge-carrier mobility was characterized by fabricating thin-film OFET devices with a bottom-gate top-contact configuration to assess the influence of aggregation on charge transport properties. In order to optimize the device performance, the thin films were annealed at different temperatures (Table S2). Clear *p*-channel OFET responses are observed for 1Py-IID and 2Py-IID (Figure 5a), and the hole mobility increases from 8.87×10^{-4} cm^2 V^{-1} s^{-1} to 7.53×10^{-3} cm^2 V^{-1} s^{-1} for 1Py-IID and 4.15×10^{-3} cm^2 V^{-1} s^{-1} to 4.74×10^{-2} cm^2 V^{-1} s^{-1} for 2Py-IID when the annealing temperature varies from 60 °C to 90 °C (Figure 5b). When the annealing temperature is increased to 120 °C (Table S2), steep drops in hole mobility are observed for both 1Py-IID and 2Py-IID, which can be ascribed to the deformation of the semiconductor layer during the post-annealing process.[16] As the annealing temperature increases to 150 °C, the OFET devices based on 1Py-IID and 2Py-IID cannot work at all. In contrast, APD-IID yields better device performance with hole mobilities of about 7.13×10^{-2} cm^2 V^{-1} s^{-1} at the annealing temperature of 60 °C. The hole mobilities can be further improved to 0.20 cm^2 V^{-1} s^{-1} along with high on/off current ratios (I_{on}/I_{off}) of $\sim10^6$ under the annealing temperature of 120 °C. While the annealing temperature reaches 150 °C, the hole mobility of APD-IID drops to 4.40×10^{-2} cm^2 V^{-1} s^{-1}. Therefore, the highest hole mobility of APD-IID is one to two orders of magnitude higher than that of 1Py-IID and 2Py-IID, which results from the better aggregation of APD-IID in the solid state. The change from benzenoid pyrene to charge-separated APD leads to stronger intermolecular interactions and better OFET performance.

In summary, we have for the first time employed nonbenzenoid APD as a building block to construct a D-A-D type semiconducting material (APD-IID), and revealed its superiority over its benzenoid isomers (1Py-IID and 2Py-IID) for electronic applications. The charge separation character of APD brings about enhanced intermolecular interactions, which prompts a more ordered packing structure. As a consequence, APD-IID exhibits one to two orders of magnitude higher mobility than that of the pyrene-based counterparts. These results demonstrate the great potential of APD as a novel building block for organic semiconducting materials. More importantly, the comparison of APD-IID and its benzenoid isomers illustrates the advantages of nonbenzenoid PAHs, and would provide new opportunities for the development of optoelectronic materials.

Acknowledgements

We are grateful to the financial support from the National Natural Science Foundation of China (Nos. 22071120, and 92256304), the National Key R&D Program of China (2020YFA0711500), and the Fundamental Research Funds for the Central Universities.

Keywords:

Nonbenzenoid arenes • Acepleiadylene • Semiconductors • Donor-acceptor systems • Aggregation

Reference

[1] (a) Y. Fei, J. Liu, *Adv. Sci.* **2022**, *9*, 2201000; (b) S. N. Spisak, Z. Zhou, S. Liu, Q. Xu, Z. Wei, K. Kato, Y. Segawa, K. Itami, A. Y. Rogachev, M. A. Petrukhina, *Angew. Chem. Int. Ed.* **2021**, *60*, 25445-25453; (c) A. Konishi, M. Yasuda, *Chem. Lett.* **2021**, *50*, 195-212; (d) K. Kato, K. Takaba, S. Maki-Yonekura, N. Mitoma, Y. Nakanishi, T. Nishihara, T. Hatakeyama, T. Kawada, Y. Hijikata, J. Pirillo, L. T. Scott, K. Yonekura, Y. Segawa, K. Itami, *J. Am. Chem. Soc.* **2021**, *143*, 5465-5469; (e) Q. Fan, L. Yan, M. W. Tripp, O. Krejčí, S. Dimosthenous, S. R. Kachel, M. Chen, A. S. Foster, U. Koert, P. Liljeroth, J. M. Gottfried, *Science* **2021**, *372*, 852-856; (f) Chaolumen, I. A. Stepek, K. E. Yamada, H. Ito, K. Itami, *Angew. Chem. Int. Ed.* **2021**, *60*, 23508-23532; (g) S. H. Pun, Q. Miao, *Acc. Chem. Res.* **2018**, *51*, 1630-1642; (h) A. Konishi, K. Horii, M. Yasuda, *J. Phys. Org. Chem.* **2023**, *36*, e4495; (i) J. Terence Blaskovits, M. H. Garner, C. Corminboeuf, *Angew. Chem. Int. Ed.* **2023**, *62*, e202218156.

[2] (a) A. Ong, T. Tao, Q. Jiang, Y. Han, Y. Ou, K.-W. Huang, C. Chi, *Angew. Chem. Int. Ed.* **2022**, *61*, e202209286; (b) L. Yang, Y.-Y. Ju, M. A. Medel, Y. Fu, H. Komber, E. Dmitrieva, J.-J. Zhang, S. Obermann, A. G. Campaña, J. Ma, X. Feng, *Angew. Chem. Int. Ed.* **2023**, *62*, e202216193; (c) P. Mathey, F. Lirette, I. Fernández, L. Renn, T. Weitz, J.-F. Morin, *Angew. Chem. Int. Ed.* **2023**, *62*, e202216281; (d) F. Wu, J. Ma, F. Lombardi, Y. Fu, F. Liu, Z. Huang, R. Liu, H. Komber, D. I. Alexandropoulos, E. Dmitrieva, T. G. Lohr, N. Israel, A. A. Popov, J. Liu, L. Bogani, X. Feng, *Angew.*

Chem. Int. Ed. **2022**, *61*, e202202170; (e) Y. Wang, Y. Huang, T. Huang, J. Zhang, T. Luo, Y. Ni, B. Li, S. Xie, Z. Zeng, *Angew. Chem. Int. Ed.* **2022**, *61*, e202200855; (f) S. Wang, M. Tang, L. Wu, L. Bian, L. Jiang, J. Liu, Z.-B. Tang, Y. Liang, Z. Liu, *Angew. Chem. Int. Ed.* **2022**, *61*, e202205658; (g) A. Shimizu, T. Morikoshi, K. Sugisaki, D. Shiomi, K. Sato, T. Takui, R. Shintani, *Angew. Chem. Int. Ed.* **2022**, *61*, e202205729; (h) K. Horii, R. Kishi, M. Nakano, D. Shiomi, K. Sato, T. Takui, A. Konishi, M. Yasuda, *J. Am. Chem. Soc.* **2022**, *144*, 3370-3375; (i) Y. Zou, Y. Han, S. Wu, X. Hou, C. H. E. Chow, J. Wu, *Angew. Chem. Int. Ed.* **2021**, *60*, 17654-17663; (j) B. Li, C. Yang, X. Wang, G. Li, W. Peng, H. Xiao, S. Luo, S. Xie, J. Wu, Z. Zeng, *Angew. Chem. Int. Ed.* **2021**, *60*, 19790-19796; (k) Y. Fei, Y. Fu, X. Bai, L. Du, Z. Li, H. Komber, K.-H. Low, S. Zhou, D. L. Phillips, X. Feng, J. Liu, *J. Am. Chem. Soc.* **2021**, *143*, 2353-2360; (l) C. Zhu, K. Shoyama, F. Würthner, *Angew. Chem. Int. Ed.* **2020**, *59*, 21505-21509; (m) J. Ma, Y. Fu, E. Dmitrieva, F. Liu, H. Komber, F. Hennersdorf, A. A. Popov, J. J. Weigand, J. Liu, X. Feng, *Angew. Chem. Int. Ed.* **2020**, *59*, 5637-5642; (n) Y. Han, Z. Xue, G. Li, Y. Gu, Y. Ni, S. Dong, C. Chi, *Angew. Chem. Int. Ed.* **2020**, *59*, 9026-9031; (o) S. H. Pun, Y. Wang, M. Chu, C. K. Chan, Y. Li, Z. Liu, Q. Miao, *J. Am. Chem. Soc.* **2019**, *141*, 9680-9686; (p) A. Konishi, Y. Okada, R. Kishi, M. Nakano, M. Yasuda, *J. Am. Chem. Soc.* **2019**, *141*, 560-571; (q) Chaolumen, H. Ito, K. Itami, *Chem. Commun.* **2019**, *55*, 9606-9609; (r) X.-S. Zhang, Y.-Y. Huang, J. Zhang, W. Meng, Q. Peng, R. Kong, Z. Xiao, J. Liu, M. Huang, Y. Yi, L. Chen, Q. Fan, G. Lin, Z. Liu, G. Zhang, L. Jiang, D. Zhang, *Angew. Chem. Int. Ed.* **2020**, *59*, 3529-3533; (s) J. Wang, F. G. Gámez, J. Marín-Beloqui, A. Diaz-Andres, X. Miao, D. Casanova, J. Casado, J. Liu, *Angew. Chem. Int. Ed.* **2023**, *62*, e202217124; (t) Y. Liang, S. Wang, M. Tang, L. Wu, L. Bian, L. Jiang, Z.-B. Tang, J. Liu, A. Guan, Z. Liu, *Angew. Chem. Int. Ed.* **2023**, *62*, e202218839; (u) T. Ikai, K. Oki, S. Yamakawa, E. Yashima, *Angew. Chem. Int. Ed.* **2023**, *62*, e202301836; (v) Y.-Y. Huang, B. Wu, D. Shi, D. Liu, W. Meng, J. Ma, L. Qin, C. Li, G. Zhang, X.-S. Zhang, D. Zhang, *Angew. Chem. Int. Ed.* **2023**, *62*, e202300990.

[3] (a) S. Mishra, T. G. Lohr, C. A. Pignedoli, J. Liu, R. Berger, J. I. Urgel, K. Müllen, X. Feng, P. Ruffieux, R. Fasel, *ACS Nano* **2018**, *12*, 11917-11927; (b) B. Mallada, B. de la Torre, J. I. Mendieta-Moreno, D. Nachtigallová, A. Matěj, M. Matoušek, P. Mutombo, J. Brabec, L. Veis, T. Cadart, M. Kotora, P. Jelínek, *J. Am. Chem. Soc.* **2021**, *143*, 14694-14702; (c) S. Mishra, D. Beyer, R. Berger, J. Liu, O. Gröning, J. I. Urgel, K. Müllen, P. Ruffieux, X. Feng, R. Fasel, *J. Am. Chem. Soc.* **2020**, *142*, 1147-1152; (d) T. G. Lohr, J. I. Urgel, K. Eimre, J. Liu, M. Di Giovannantonio, S. Mishra, R. Berger, P. Ruffieux, C. A. Pignedoli, R. Fasel, X. Feng, *J. Am. Chem. Soc.* **2020**, *142*, 13565-13572.

[4] (a) Y. Zou, W. Zeng, T. Y. Gopalakrishna, Y. Han, Q. Jiang, J. Wu, *J. Am. Chem. Soc.* **2019**, *141*, 7266-7270; (b) X. Yang, F. Rominger, M. Mastalerz, *Angew. Chem. Int. Ed.* **2019**, *58*, 17577-17582; (c) X. Lu, T. Y. Gopalakrishna, Y. Han, Y. Ni, Y. Zou, J. Wu, *J. Am. Chem. Soc.* **2019**, *141*, 5934-5941.

[5] (a) Z.-L. Qiu, X.-W. Chen, Y.-D. Huang, R.-J. Wei, K.-S. Chu, X.-J. Zhao, Y.-Z. Tan, *Angew. Chem. Int. Ed.* **2022**, *61*, e202116955; (b) J. Liu, S. Mishra, C. A. Pignedoli, D. Passerone, J. I. Urgel, A. Fabrizio, T. G. Lohr, J. Ma, H. Komber, M. Baumgarten, C. Corminboeuf, R. Berger, P. Ruffieux, K. Müllen, R. Fasel, X. Feng, *J. Am. Chem. Soc.* **2019**, *141*, 12011-12020; (c) A. Konishi, K. Horii, D. Shiomi, K. Sato, T. Takui, M. Yasuda, *J. Am. Chem. Soc.* **2019**, *141*, 10165-10170.

[6] (a) C. Duan, J. Zhang, J. Xiang, X. Yang, X. Gao, *Angew. Chem. Int. Ed.* **2022**, *61*, e202201494; (b) M. A. Medel, R. Tapia, V. Blanco, D. Miguel, S. P. Morcillo, A. G. Campaña, *Angew. Chem. Int. Ed.* **2021**, *60*, 6094-6100; (c) M. A. Medel, C. M. Cruz, D. Miguel, V. Blanco, S. P. Morcillo, A. G. Campaña, *Angew. Chem. Int. Ed.* **2021**, *60*, 22051-22056; (d) N. Ogawa, Y. Yamaoka, H. Takikawa, K.-i. Yamada, K. Takasu, *J. Am. Chem. Soc.* **2020**, *142*, 13322-13327.

[7] (a) H. Xin, X. Gao, *ChemPlusChem* **2017**, *82*, 945-956; (b) H. Xin, B. Hou, X. Gao, *Acc. Chem. Res.*

2021, *54*, 1737-1753; (c) J. Huang, S. Huang, Y. Zhao, B. Feng, K. Jiang, S. Sun, C. Ke, E. Kymakis, X. Zhuang, *Small Methods* **2020**, *4*, 2000628.

[8] (a) J. Yao, Z. Cai, Z. Liu, C. Yu, H. Luo, Y. Yang, S. Yang, G. Zhang, D. Zhang, *Macromolecules* **2015**, *48*, 2039-2047; (b) H. Xin, C. Ge, X. Yang, H. Gao, X. Yang, X. Gao, *Chem. Sci.* **2016**, *7*, 6701-6705; (c) Y. Yamaguchi, M. Takubo, K. Ogawa, K.-i. Nakayama, T. Koganezawa, H. Katagiri, *J. Am. Chem. Soc.* **2016**, *138*, 11335-11343; (d) H. Xin, C. Ge, X. Jiao, X. Yang, K. Rundel, C. R. McNeill, X. Gao, *Angew. Chem. Int. Ed.* **2018**, *57*, 1322-1326; (e) H. Xin, J. Li, C. Ge, X. Yang, T. Xue, X. Gao, *Mater. Chem. Front.* **2018**, *2*, 975-985; (f) J. Wang, M. Chu, J.-X. Fan, T.-K. Lau, A.-M. Ren, X. Lu, Q. Miao, *J. Am. Chem. Soc.* **2019**, *141*, 3589-3596; (g) B. Hou, J. Li, Z. Zhou, W. L. Tan, X. Yang, J. Zhang, C. R. McNeill, C. Ge, J. Wang, X. Gao, *ACS Macro Lett.* **2022**, *4*, 392-400.

[9] E. Puodziukynaite, H.-W. Wang, J. Lawrence, A. J. Wise, T. P. Russell, M. D. Barnes, T. Emrick, *J. Am. Chem. Soc.* **2014**, *136*, 11043-11049.

[10] T. Tang, A. K. K. Kyaw, Q. Zhu, J. Xu, *Chem. Commun.* **2020**, *56*, 9388-9391.

[11] P. Liu, X.-Y. Chen, J. Cao, L. Ruppenthal, J. M. Gottfried, K. Müllen, X.-Y. Wang, *J. Am. Chem. Soc.* **2021**, *143*, 5314-5318.

[12] (a) M. Li, H. Fu, B. Wang, J. Cheng, W. Hu, B. Yin, P. Peng, S. Zhou, X. Gao, C. Jia, X. Guo, *J. Am. Chem. Soc.* **2022**, *144*, 20797-20803; (b) H. Dong, X. Fu, J. Liu, Z. Wang, W. Hu, *Adv. Mater.* **2013**, *25*, 6158-6183.

[13] (a) T. M. Figueira-Duarte, K. Müllen, *Chem. Rev.* **2011**, *111*, 7260-7314; (b) F. Xie, X. Yang, P. Jin, X.-T. Wang, H. Ran, H. Zhang, H. Sun, S.-J. Su, J.-Y. Hu, *Adv. Optical Mater.* **2022**, 2202490; (c) Y. Yu, P. Xu, Y. Pan, X. Qiao, L. Ying, D. Hu, D. Ma, Y. Ma, *Adv. Optical Mater.* **2022**, 2202217; (d) J. Zeng, N. Qiu, J. Zhang, X. Wang, C. Redshaw, X. Feng, J. W. Y. Lam, Z. Zhao, B. Z. Tang, *Adv. Optical Mater.* **2022**, *10*, 2200917.

[14] (a) F. Würthner, *Acc. Chem. Res.* **2016**, *49*, 868-876; (b) C. Zhang, J. Cheng, Q. Wu, S. Hou, S. Feng, B. Jiang, C. J. Lambert, X. Gao, Y. Li, J. Li, *J. Am. Chem. Soc.* **2023**, *145*, 1617-1630; (c) D. Bischof, M. W. Tripp, S. I. Ivlev, U. Koert, G. Witte, *Cryst. Growth Des.* **2022**, *22*, 6857-6862; (d) R. G. Huber, M. A. Margreiter, J. E. Fuchs, S. von Grafenstein, C. S. Tautermann, K. R. Liedl, T. Fox, *J. Chem. Inf. Model.* **2014**, *54*, 1371-1379.

[15] C. He, Q. He, Q. Chen, L. Shi, H. Cao, J. Cheng, C. Deng, T. Lin, *Tetrahedron Lett.* **2010**, *51*, 1317-1321.

[16] Y. Yamaguchi, Y. Kojiguchi, S. Kawata, T. Mori, K. Okamoto, M. Tsutsui, T. Koganezawa, H. Katagiri, T. Yasuda, *Chem. Mater.* **2020**, *32*, 5350-5360.

[17] (a) Z.-F. Yao, Z.-Y. Wang, H.-T. Wu, Y. Lu, Q.-Y. Li, L. Zou, J.-Y. Wang, J. Pei, *Angew. Chem. Int. Ed.* **2020**, *59*, 17467–17471; (b) H.-T. Wu, Z.-F. Yao, Z. Xu, H.-K. Kong, X.-Y. Wang, Q.-Y. Li, J.-Y. Wang, J. Pei, *Macromol. Rapid Commun.* **2022**, *43*, 2200069.

[18] (a) H. Sirringhaus, P. J. Brown, R. H. Friend, M. M. Nielsen, K. Bechgaard, B. M. W. Langeveld-Voss, A. J. H. Spiering, R. A. J. Janssen, E. W. Meijer, P. Herwig, D. M. de Leeuw, *Nature* **1999**, *401*, 685-688; (b) M. E. Gemayel, K. Börjesson, M. Herder, D. T. Duong, J. A. Hutchison, C. Ruzié, G. Schweicher, A. Salleo, Y. Geerts, S. Hecht, E. Orgiu, P. Samorì, *Nat. Commun.* **2015**, *6*, 6330.